American Journal of Engineering and Applied Sciences

Original Research Paper

Fast and Robust Maximum Power Point Tracking for Solar Photovoltaic Systems

[1]Huiying Zheng and [2]Shuhui Li

[1]*Process Automation Solutions - an ATS Company, Bessermer, AL, USA*
[2]*Department of Electrical and Computer Engineering, The University of Alabama, Tuscaloosa AL, USA*

Article history
Received: 04-12-2015
Revised: 12-01-2016
Accepted: 13-01-2016

Corresponding Author:
Shuhui Li
Department of Electrical and Computer Engineering, The University of Alabama, Tuscaloosa, USA
Email: sli@eng.ua.edu

Abstract: Solar Photovoltaic (PV) energy is becoming an increasingly important part of the world's renewable energy. In order to develop technology for efficient energy conversion from a solar PV system, this paper studies typical Maximum Power Point Tracking (MPPT) control techniques used in solar PV industry and then proposes a close-loop and adaptive MPPT method for reliable and rapid extraction of solar PV power. The paper emphasizes especially on how the proposed and conventional adaptive MPPT methods perform under highly variable weather and solar irradiation conditions in a digital control environment. A computer simulation system is developed by using SimPowerSystems and Opal-RT real-time simulation technology which allows for fast and efficient investigations of the MPPT algorithms under high switching frequency conditions for power converters. A hardware experiment system is built to validate and compare the proposed and conventional MPPT techniques in a more practical condition. Advantages, disadvantages and properties of different MPPT methods are compared and studied, evaluated.

Keywords: Solar PV Array, Maximum Power Point Tracking, Digital Control, Computational and Hardware-Based Experiments

Introduction

Photovoltaic (PV) systems can be easily integrated in residential buildings, hence they will be the main responsibility of making low-voltage grid power flow bidirectional (Mastromauro *et al*., 2012). A grid-connected solar PV system consists of a PV generator that produces electricity from sunlight and power converters for energy extraction and grid-interface (Lorenzo *et al*., 1994; Carrasco *et al*., 2006; Nelson, 2003). The main applications of PV systems are in stand-alone (Joerissen *et al*., 2004; Masters, 2004) or grid-connected configurations (Chedid *et al*., 1998). In the stand-alone configuration, a PV system is disconnected from the grid and its generated power is either stored in an energy storage device or consumed by loads connected to it. In the grid-connected configuration, however, the power captured by a PV system can be both delivered to the grid and consumed by loads.

A PV generation system has two major weaknesses: (1) Low energy conversion efficiency (9-17%) (Faranda and Leva, 2008), particularly at a low solar irradiation level; (2) the amount of electric power captured by a PV generator varies constantly with weather conditions. The captured power of a PV system depends on the temperature and solar irradiance. Generally, there is a unique point, called the Maximum Power Point (MPP), at which the whole PV system operates with maximum efficiency and produces its maximum output power. The location of the MPP is unknown, but can be located through a searching algorithm. To maximize the output power of a PV system, continuously tracking the MPP of the PV system is essential.

Many different approaches have been proposed to maximize the power capture from a PV generator. Typical MPPT techniques that have been proposed in the literature comprise of the Short-Circuit Current (Noguchi *et al*., 2002), Open-Circuit Voltage (Kobayashi *et al*., 2004), Perturb and Observe (P&O) (Mastromauro *et al*., 2012; Faranda *et al*., 2008; Al-Amoudi and Zhang, 1998), Incremental Conductance (IC) (Mastromauro *et al*., 2012; Femia *et al*., 2006; Wu *et al*., 2003), Adaptive P&O (Szabados and Wu, 2008; Femia *et al*., 2005) and Intelligent and Fuzzy Logic methods (Veerachary *et al*., 2003; Khaehintung *et al*., 2004). These methods vary between each other in numerous respects, including convergence speed, simplicity, stability and tracking efficiency.

The primary challenges for the MPPT of a solar PV array include: (1) How to get to a MPP quickly, (2) how to stabilize at a MPP and (3) how to make a smooth transition from one MPP to another under sharply changing weather conditions. In general, a fast and reliable MPPT is critical for power generation from a solar PV system. In order for effective development and design of solar PV systems, it is essential to investigate and compare performance, operating principles and advantages or disadvantages of conventional MPPT techniques used in the solar PV industry and develop new competent technology for fast and reliable extraction of solar PV power.

In the following sections, the paper first presents a brief analysis about PV array characteristics and how the PV array characteristics are affected by temperature and solar irradiance in section 2. Section 3 examines conventional fixed-step MPPT approaches used in solar PV industry. Section 4 presents traditional adaptive MPPT techniques and a proposed Proportional-Integral (PI) based adaptive MPPT approach for fast and reliable tracking of PV array maximum power. Section 5 gives computer simulation evaluation of the proposed and conventional MPPT methods under stable and variable weather conditions. Section 6 shows a hardware experiment evaluation of the conventional and proposed MPPT methods under actual power converter operating conditions in a dSPACE-based digital control environment. Finally, the paper concludes with the summary of main points.

Extracted Power Characteristics

A grid-connected solar PV system consists of three parts (Fig. 1): An array of photovoltaic cells, power electronic converters and an integrated control system (Kobayashi *et al*., 2004; Faranda *et al*., 2008). The control system of a solar PV array contains two parts: One for MPPT and the other for grid interface (Wu *et al*., 2003; Szabado and Wu, 2008; Femia *et al*., 2005; Veerachary *et al*., 2003). Both control functions are achieved through power electronic converters. Overall, the dc/dc converter performs the MPPT function while the dc/ac converter implements the grid interface control.

Figure 2 illustrates typical *I-V* and *P-V* characteristics of a PV array for two different irradiance levels. As shown by the figure, if the output voltage of the dc/dc converter applied to the PV array is low, the output current of the PV array is almost constant for a given irradiation level. As the voltage applied to the PV array goes up, the power outputted from the PV array increases. When the output power of the PV array reaches the maximum value, an increase of the applied voltage would cause the output current of the PV array to drop radically and the output power decreases. During a day, solar irradiation and temperature rise and fall over time (ATSRD, 2011), which causes the continuous alteration of the MPP of the PV array. Thus, in order to collect the maximum available power, the operating point needs to be tracked continuously using a MPPT algorithm (Mastromauro *et al*., 2012).

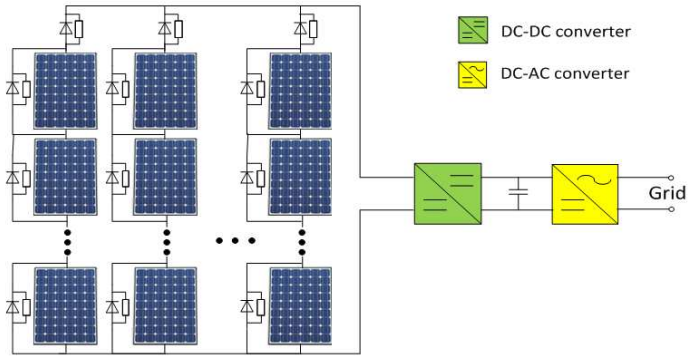

Fig. 1. Configuration of grid-tied solar PV system

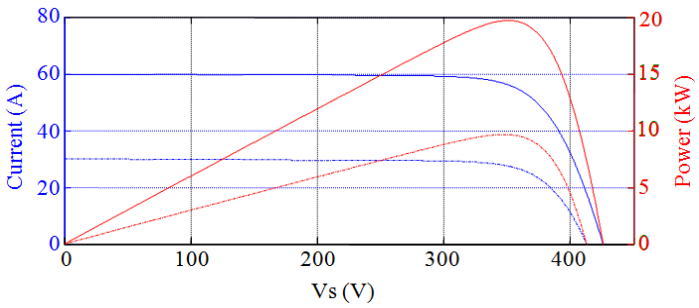

Fig. 2. Solar PV array characteristics

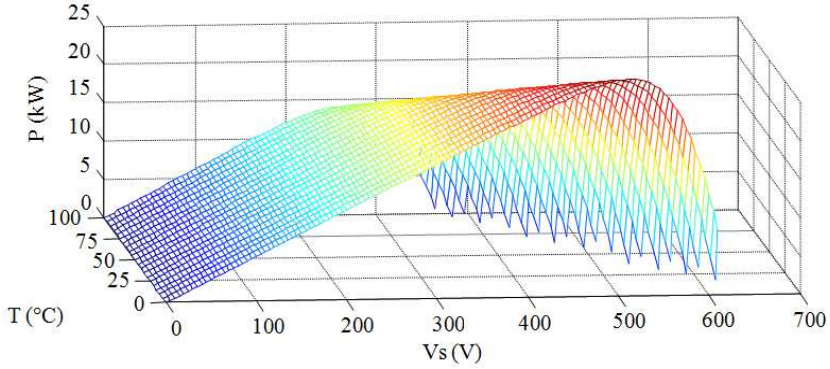

Fig. 3. Output power characteristics of a PV array versus temperature and voltage

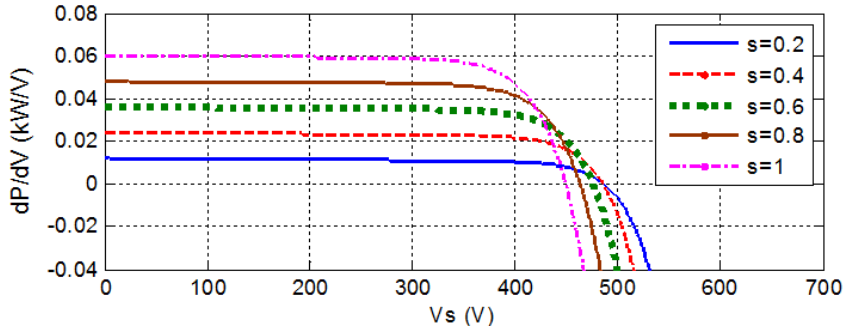

Fig. 4. Derivative of power over applied voltage to a PV array under different irradiation

Figure 3 and 4 demonstrate the impact of temperature and solar irradiation to the power production of a PV array. According to Fig. 3, as the temperature increases, the maximum power captured by the PV array drops and the MPP voltage reduces indicating that a PV array produces more power on a cold day than a hot one. Regarding solar irradiation, a change of the solar irradiation level could affect both photo-generated current and temperature of PV cells within a PV array. Figure 4 shows the derivative of PV array output power versus the voltage applied to the PV array for several constant irradiance levels. In the figure, *S* represents the ratio of the solar irradiance over the nominal irradiance of 1000 W/m^2. For each constant irradiance intensity, the applied voltage to the PV array at the zero derivative is the required MPP voltage. The zero derivative points represent the location of MPPs. According to Fig. 4, for each irradiance intensity, the derivative is positive before reaching the MPP and negative after the MPP. As the irradiation level changes, the zero derivative point shifts a little bit to the left or right due to the temperature impact of irradiance intensity on PV cells.

Conventional MPPT Strategies

Many different MPPT methods have been proposed for energy extraction from PV generators. Typical MPPT techniques consist of Short-Circuit Current (SCC) (Noguchi *et al*., 2002), Open-Circuit Voltage (OCV) (Kobayashi *et al*., 2004), P&O (Faranda *et al*., 2008; Al-Amoudi and Zhang, 1998) and IC methods (Femia *et al*., 2006; Wu *et al*., 2003). Among all, P&O and IC techniques are the most broadly adopted approaches for MPPT control of a PV array (Mastromauro *et al*., 2012).

Perturb and Observe Method

The P&O technique is the most widely used MPPT method for PV arrays. It operates by periodically perturbing the voltage applied to a PV array and comparing the output power of the PV array with that of the previous perturbation cycle. In general, if an increase of the voltage applied to the PV array causes an increase of the output power, the P&O controller moves the operating point along that direction; otherwise the perturbation is adjusted to the reverse direction. The P&O process continues until a MPP is reached (Esram and Chapman, 1995; Abdelsalam and Massoud, 2011; Faranda *et al*., 2008). Many different P&O methods have been reported in the literature. In classic P&O methods (Al-Amoudi and Zhang, 1998), the perturbation of the voltage applied to a PV array has a fixed value. In the optimized P&O methods (Esram and Chapman, 1995;

Abdelsalam and Massoud, 2011), an average of multiple samples of the array output power is used to determine the perturbation magnitude for improved MPPT. In (Femia *et al*., 2009), a compensation network is used to improve P&O stability.

Incremental Conductance Method

The IC method is developed based on the principle that at the MPP, the following equation holds (Femia *et al*., 2006; Faranda *et al*., 2008):

$$dI_a/dV_a + I_a/V_a = 0 \quad (1)$$

Also, if the operating point of the *PV* generator is on the right of the MPP, $dI_a/dV_a + I_a/V_a < 0$; if the operating point is on the left of the MPP, $dI_a/dV_a + I_a/V_a > 0$. Hence, the direction to perturb the MPP operating point of the *PV* generator can be determined by comparing the instant conductance I_a/V_a with the incremental conductance dI_a/dV_a (Fig. 5). Using the IC method, it is theoretically possible to know when to stop the perturbation process as the MPP is reached.

Fast and Reliable Adaptive MPPT Techniques

In a PV system, the tracking speed and accuracy are the key factors for the MPPT control. These factors directly relate to the duty ratio adjustment of the dc/dc converter. Since conventional MPPT algorithms are unable to meet those requirements (Otieno *et al*., 2009; Yu, 2007), adaptive MPPT approaches have been proposed recently, including fuzzy logic based MPPT (Veerachary *et al*., 2003; Khaehintung *et al*., 2004), neural networks MPPT (Hussein *et al*., 2002; Sun *et al*., 2002) and ripple correlation control MPPT (Midya *et al*., 1996), etc. All of them basically belong to a "discrete" adaptive MPPT technique.

Traditional Adaptive MPPT Methods

In conventional adaptive MPPT methods, the perturbation magnitude varies during the MPP tracking process (Femia *et al*., 2005; Esram and Chapman, 1995). Typical adaptive P&O techniques utilize the derivative of power vs. PV array terminal voltage to determine next perturbation action. This is based on the analysis that the derivative is positive on the left of the MPP, zero at the MPP and negative on the right of the MPP as shown by Fig. 4. Therefore, (Esram and Chapman, 1995) proposed a Scaling Factor (SF) perturbation technique as shown by (2), in which M is a constant coefficient and the duty ratio in the next perturbation cycle is determined by the multiplication of M with the derivative. Hence, the duty ratio adjustment is scalable rather than fixed. Similar to the IC technique, the perturbation process stops theoretically as the MPP is reached:

$$d(k) = d(k-1) - M\frac{dP_a}{dV_a} \quad (2)$$

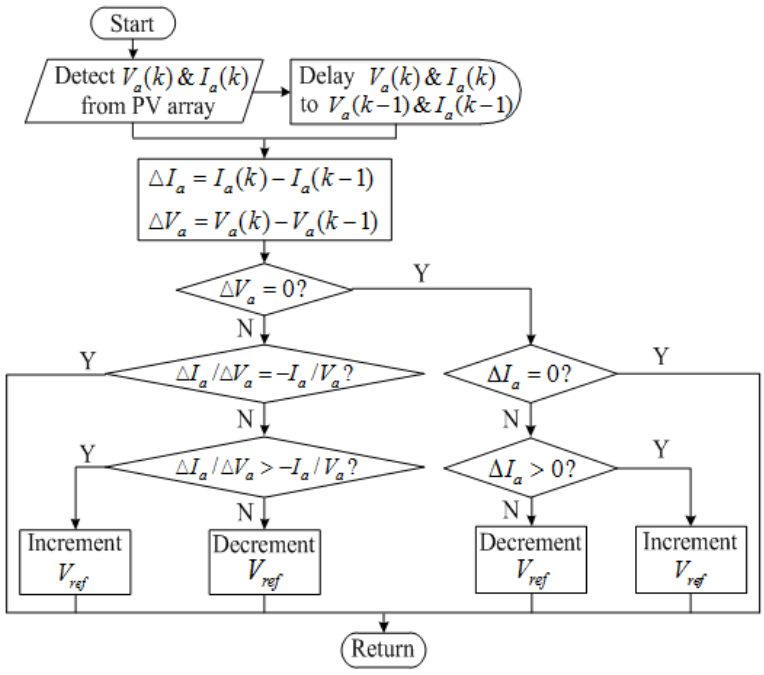

Fig. 5. Flowchart of the incremental conductance algorithm

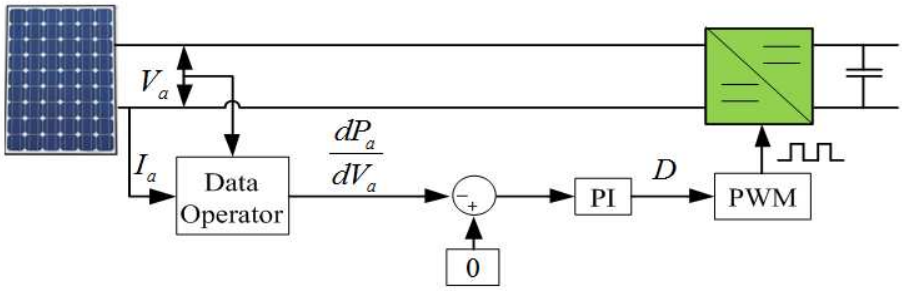

Fig. 6. PI based MPPT control loop diagram of the PV system

Another conventional adaptive duty ratio strategy is based on a Proportional-Integral (PI) control mechanism (Fig. 6). The error signal to the controller is generated by comparing dP_a/dV_a with a zero power derivative reference value. The duty ratio of the dc/dc converter is regulated continuously until the MPP is reached, i.e., $dP_a/dV_a = 0$. This inner close-loop control structure has a much faster response speed than the open-loop regulation mechanism used in P&O and IC methods so that a rapid MPP tracking can be achieved. However, a major problem for his control structure is that for a high $|dP_a/dV_a|$, the fast close-loop regulation of the duty-ratio could reduce the MPPT efficiency and cause more oscillation in the output power.

Proposed Hyperbolic-PI (H-PI) Adaptive MPPT Method

The proposed adaptive MPPT strategy has adopted the advantage of the inner close-loop control mechanism for the duty-ratio regulation. But, it introduces a hyperbolic function (3) into the MPPT design:

$$y = \tanh\left(k \cdot dP_a/dV_a\right) \tag{3}$$

In (3), k is a constant and is tuned to meet a reliable and fast MPPT requirement for a typical solar PV array. The output of the hyperbolic function is close to 1 if $|dP_a/dV_a|$ is large but reduces greatly if $|dP_a/dV_a|$ is small. This hyperbolic function allows for a more stable and accurate and much faster MPP tracking properties under dynamic condition. The control diagram of the proposed H-PI method is shown by Fig. 7, the measured current and voltage are first processed by a low-pass filter. After that, the derivative of power vs. voltage passes through a hyperbolic function and the amount of the duty-ratio adjustment is determined through a PI controller which generates a new duty-ratio and applies it to the dc/dc converter for the next control cycle.

One issue for the proposed MPPT is the computation associated with tanh(•) function. In general, the tanh(•) can be calculated very quickly in a digital control system. According to a large number of experiments performed over a 2GHz PC, the average computation time of tanh(•) in MatLab is about 10ns. Compared to the controller sampling time, the computation time of tanh(•) is much smaller and ignorable. For tanh(•) implementation in a DSP chip, the additional computational effort is even more insignificant.

MPP Tracking Analysis of Conventional and Proposed Adaptive MPPT Methods

How to process the derivative of dP_a/dV_a causes a big difference in MPP tracking using the conventional and proposed adaptive MPPT strategies. Actually, the derivative operation can cause a high non-linearity. For the conventional adaptive MPPT, this derivative is directly used to regulate the duty ratio, which could result in a large regulation of the PV array voltage and a high oscillation in the MPP tracking especially when a large derivative appears. However, for the proposed adaptive MPPT, although a sudden surge of solar irradiation level causes a sharp change in the derivative of dP_a/dV_a, the derivative is preprocessed by the hyperbolic function before it is applied to the PI controller. In general, the hyperbolic function reduces $|dP_a/dV_a|$ when a large ΔP_a and a small ΔV_a appear but increases $|dP_a/dV_a|$ when a large ΔP_a and a large ΔV_a are present. Hence, both the tracking speed and reliability are improved. The improvement is especially evident when there are fast random changes of solar irradiation or random measurement noises in the PV control system. Comprehensive simulation and hardware experiment results demonstrate that the processing through the hyperbolic function makes it much more stabile and reliable and faster for maximum power tracking of PV power (sections 5 and 6).

Computational Experiments and Analysis

To evaluate and compare different MPPT approaches, a computer simulation platform of the integrated power converter and PV array system is built. The experiment system mainly includes three parts: A PV array module, a dc/dc boost converter and a dc/ac inverter.

DOI: 10.3844/ajeassp.2016.755.769

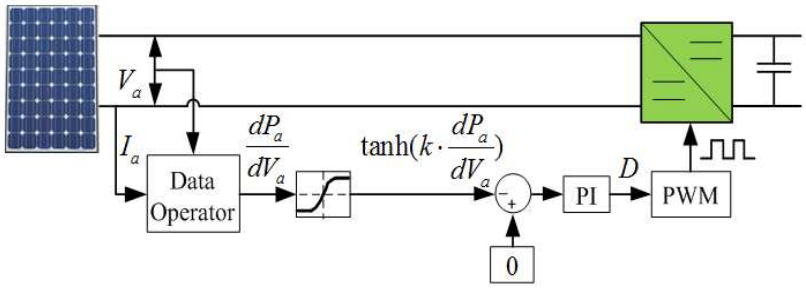

Fig. 7. Control loop diagram of proposed adaptive MPPT

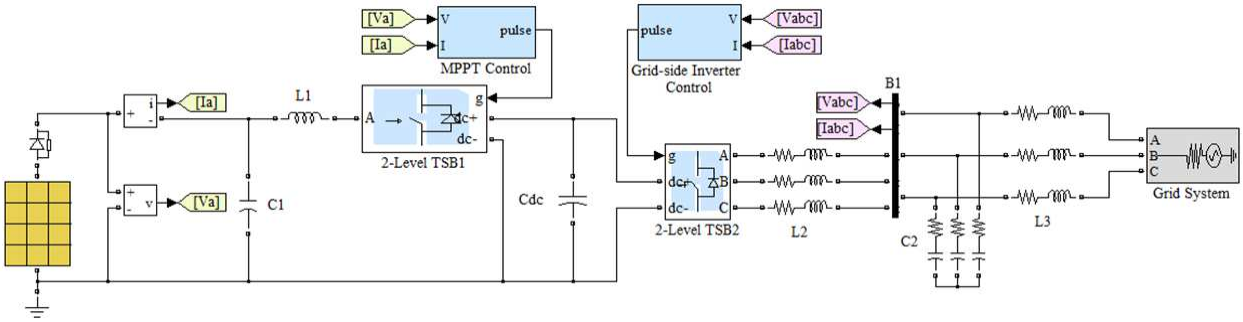

Fig. 8. Solar PV generator with the MPPT and grid-integration using SimPowerSystems and Opal-RT RT-LAB

The PV array has a series-parallel configuration comprises of 10 parallel strings with each string containing 20 series panels (Fig. 8). Each PV panel has an external bypass diode in parallel with the panel (Masters, 2004). At the top of each string, a blocking diode is included (Masters, 2004). The dc/dc boost converter is regulated by the MPPT control module for MPPT control of the PV array (Fig. 8). The dc/ac inverter integrates the PV system to the grid and an LCL filter is employed to enhance the power quality in the three-phase ac system. A direct-current vector control technique is used to control the dc/ac inverter, which consists of a d-axis loop for dc-link voltage control and a q-axis loop for grid voltage support or reactive power control. Details about the direct-current vector control is available in (Li *et al*., 2011). Major measurements of the PV generator include terminal current, voltage and output power of the PV array, dc-link voltage and voltage, current and power at the grid side. The generator sign convention is employed, i.e., power transferred to the grid is positive.

The converter modules are from Opal-RT RTE-Drive toolbox and can be integrated with the RTE PWM signal generation function from Opal-RT RT-EVENTS toolbox to generate converter driving pulses for very fast and precise simulation of power converters (ORTT, 2003). The switching frequencies are 10 kHz for the dc/dc converter and 1800 Hz for the dc/ac inverter, respectively and losses of the power converters and the LCL filter are included.

The development of the MPPT control module has considered digital control system natures, including digital signal processing, sample and hold and time delays (Fig. 9). The measured current and voltage signals is first processed through sample and hold blocks, which transfers measured “continuous” signals to “discrete” signals. Then, a digital filtering is utilized to eliminate high frequency components that may be caused by noises or rapid switching of power converters. A time delay block is included to simulate potential delay between digital and physical systems. The comparison focuses mainly on IC fixed step, traditional Scaling Factor (SF) adaptive and the proposed Hyperbolic-PI based (H-PI) MPPT methods.

MPPT Evaluation under Step and Ramp Changes of Solar Irradiance

Usually, temperature change smoothly during a day (ATSRD, 2011), but solar irradiance levels could vary rapidly from one value to another. To test and compare different MPPT algorithms under sharp changes of solar irradiance levels, a solar irradiance curve with step and ramp variations is generated (Fig. 10a). The irradiation has a step change from 400 to 1000 W/m^2 at 1.5 s, is kept at 1000 W/m^2 within 1.5 and 2.2 s and changes to 600 W/m^2 at 2.2s. At 2.9 s, there is a ramp change of the solar irradiance level until it reaches 900 W/m^2 at 3.2 s. Then, the solar irradiance stays at 900 W/m^2 for 0.6 s and reduces slowly to 700 W/m^2 at 4s.

DOI: 10.3844/ajeassp.2016.755.769

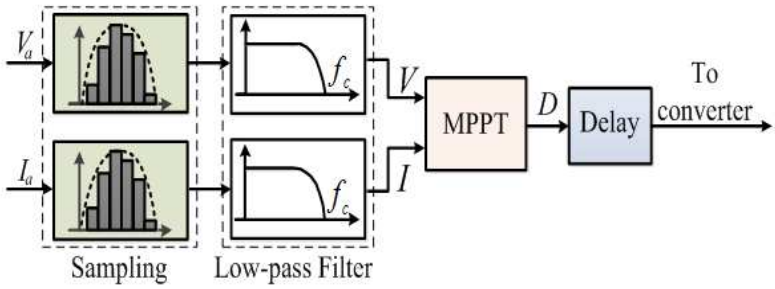

Fig. 9. MPPT digital control module

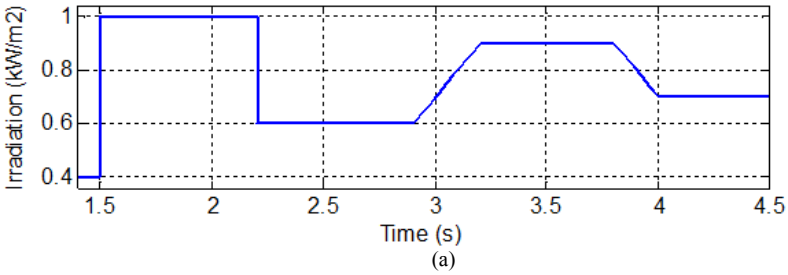

(a)

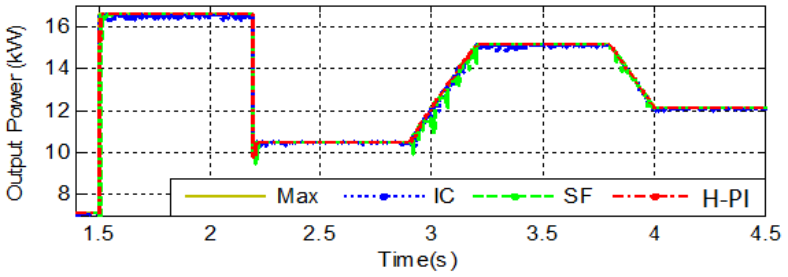

(b)

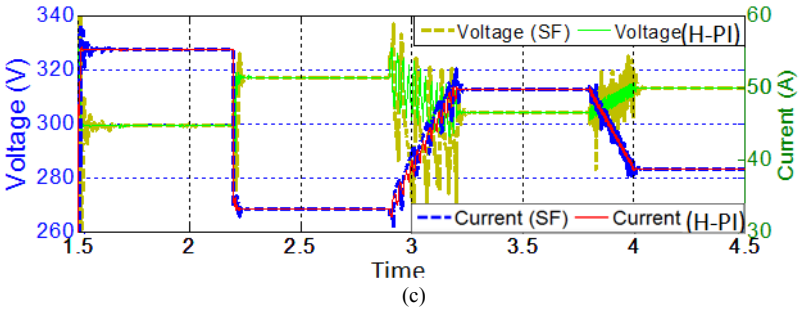

(c)

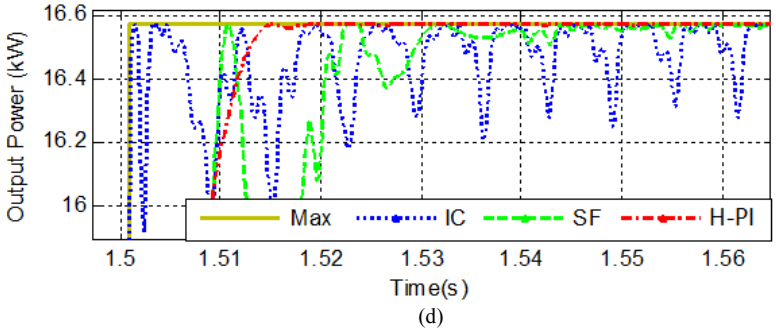

(d)

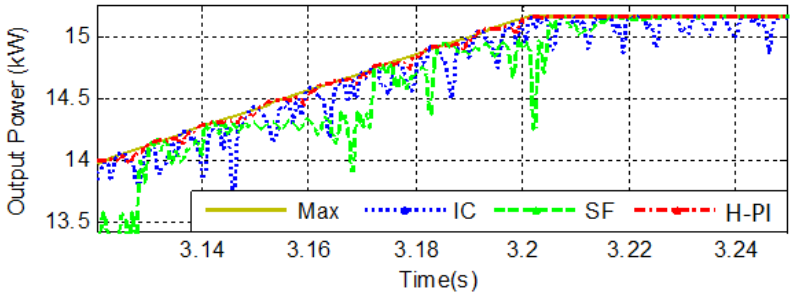
Output Power (kW)
15
14.5
14
13.5
Max
IC
SF
H-PI
3.14
3.16
3.18
3.2
3.22
3.24
Time(s)

(e)

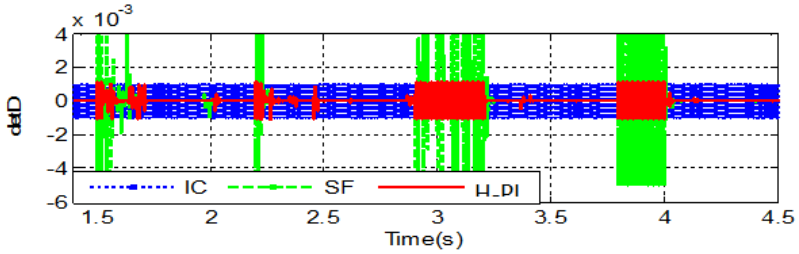
x 10^-3
4
2
0
-2
-4
-6
IC
SF
H-PI
1.5
2
2.5
3
3.5
4
4.5
Time(s)

(f)

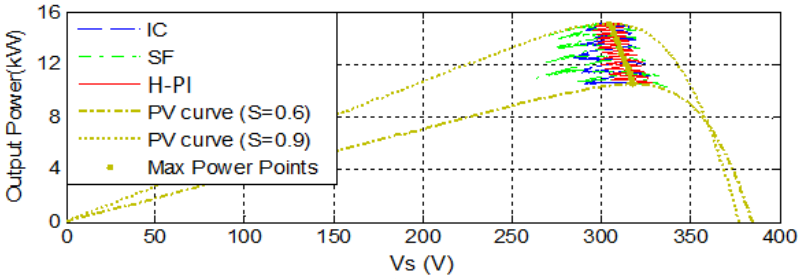
Output Power(kW)
16
12
8
4
0
IC
SF
H-PI
PV curve (S=0.6)
PV curve (S=0.9)
Max Power Points
0
50
100
150
200
250
300
350
400
Vs (V)

(g)

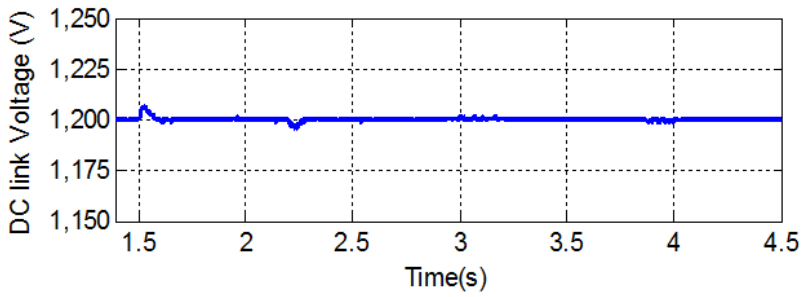
DC link Voltage (V)
1,250
1,225
1,200
1,175
1,150
1.5
2
2.5
3
3.5
4
4.5
Time(s)

(h)

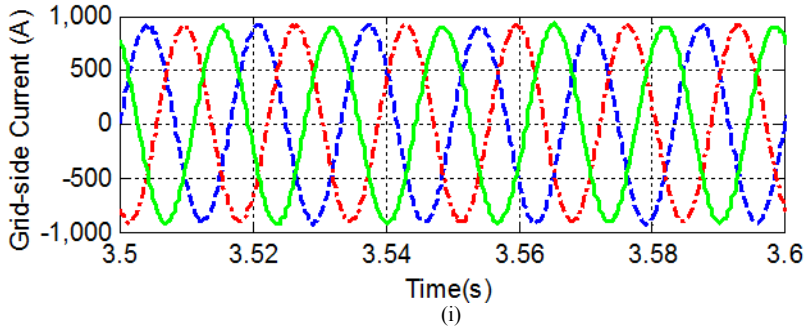
Grid-side Current (A)
1,000
500
0
-500
-1,000
3.5
3.52
3.54
3.56
3.58
3.6
Time(s)

(i)

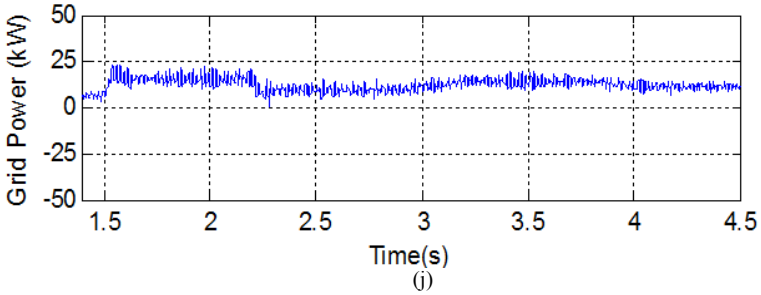

Fig. 10. Comparison of different MPPT techniques under step and ramp changes of solar irradiance levels (a) Step and ramp changes of solar irradiance levels (b) PV array maximum and output power (c) Current and voltage waveforms of SF and H-PI MPPTs (d) A zoomed in PV array maximum and output power at a step change (e) A zoomed in PV array output power at an increasing slope change (f) Changes of duty ratio (g) Power Vs. voltage locus at the increasing slope change (h) dc-link voltage (i) Three-phase grid-side currents (j) dc/ac inverter power at the grid side

The PV array maximum power, along with the captured power by using IC, SF and H-PI methods under the step/ramp changes of solar irradiance levels, is presented by Fig. 10b. The sampling rate of the MPPT controller is 0.1 ms. The current and voltage waveforms of the proposed MPPT are shown by Fig. 10c. Figure 10d and 10e are the zoom-in plots of Fig. 10b. Figure 10f presents the duty-ratio adjustment during the MPPT control. Figure 10g shows, for the three MPPT methods, the power vs. voltage locus for a slope change of the solar irradiation level from 0.6 to 0.9 kW/m^2 around 3sec (Fig. 10a).

For the IC method, it is quite stable under sharp and gradient solar irradiation changes. The primary issue of the IC method is a continuous perturbation in duty ratio (Fig. 10f) even when the solar irradiance level is stable, causing the oscillation of the captured power. The extent of the power oscillation relies on the perturbation step. The smaller the perturbation step, the smaller the oscillation. Nevertheless, if the perturbation step is too small, the MPPT speed will be affected.

For the SF method, there is a very small oscillation when the irradiation level remains at a stable level, at which the power over the voltage derivative is close to zero. But, for changing irradiation levels, the output power of the PV array oscillates a lot as demonstrated by time-domain waveforms (Fig. 10d and 10e) and the power vs. voltage locus plot (Fig. 10g). This results from a sharp change of dP_a/dV_a around the MPP (Fig. 4), causing unstable variation in duty ratio.

The proposed H-PI approach shows the best performance (Fig. 10b, d, e and g). This is due to the fact that the duty ratio adjustment of the H-PI method is tuned based on the power and voltage derivative that is preprocessed through a hyperbolic function as shown by Equation 3. As it can be seen in Fig. 10f, the change in duty ratio has a smoothly continuous value during an abrupt or ramp change of solar irradiation and is around zero when the solar irradiation is stable.

The PV voltage and current oscillate continuously (Fig. 10c), particularly under changing solar irradiation conditions. This causes more oscillation of the instantaneous power of the PV array. This issue is critical and must be considered in the design of the low-pass filters (Fig. 9) to assure fast and robust MPP tracking, particularly for the adaptive MPPT techniques (Fig. 6 and 7). The power vs. voltage locus as shown by Fig. 10g illustrates more clearly how the maximum power is tracked by using three different MPPTs approaches. As it can be seen from the figure, the proposed adaptive MPPT is more reliable and efficient in tracking the MPP than conventional adaptive MPPT.

The dc-link voltage is stable under the direct-current vector control technique applied to the dc/ac inverter, which is an important factor for the MPPT. The waveform of the three-phase current on the grid side is shown by Fig. 10i and the instantaneous grid power is shown by Fig. 10j. As shown by Fig. 10j, the grid power follows the captured PV power. However, due to the existence of harmonics and unbalance in the grid three-phase currents, there are oscillations in the grid power, which is similar to the instantaneous grid power in other renewable energy applications (Li *et al*., 2012; Bao *et al*., 2012).

Sampling Rate Impact

In design of a digital control system, sampling rate is generally predetermined. After that, the perturbation controller for each MPPT technique should be designed independently until satisfactory performance is obtained. Figure 11 shows the tracking of MPP by using the three different MPPT methods under the sampling rate of 1ms and 10 ms per sample, respectively. As shown by Fig. 11a, all the MPPT methods can track MPP when the sample time is 1ms. However, when the sample time is 10 ms, there will be a big notch in the captured power by IC and SF method (Fig. 11b). An examination of power Vs. voltage locus (Fig. 11c) reveals more detailed information about the MPP tracking using the three different MPPT approaches.

The figure, consistent with Fig. 10g, demonstrates that the proposed adaptive MPPT is more reliable. Overall, the proposed method responses much faster and is more stable under different irradiation conditions.

It is needed to point out that the sampling rate determines the waiting time for the next perturbation. From this point of view, the sampling rate concept is not exactly equivalent to the cutoff frequency notion normally used in the digital signal processing field. In a MPPT algorithm for a PV array, the low-pass filters shown in Fig. 9 help to remove noises while the sampling rate determines how fast to conduct the next perturbation. The impact of the sampling rate can be seen from Fig. 11. In general, as the sampling time increases, it is slower to track the maximum power.

MPPT under Variable Solar Irradiance Condition

In reality, solar irradiance level changes continually over time (Mills *et al*., 2011). Hence, it is important to compare and evaluate different MPPT methods under variable irradiation conditions. For this purpose, a variable solar irradiance curve is generated (Fig. 12a). Figure 12b compares the MPP tracking using different MPPT algorithms and the parameters of the MPPT algorithms are the same as those used in Fig. 10. As shown by the figure, among the three MPPT algorithms, the proposed H-PI method is the most effective to track the MPP. For the IC method, the fixed step perturbation disables the fast changing requirement in duty ratio to track the MPP. For the SF method, a stable adaptive adjustment based on the derivative information is hard to obtain in tracking the MPP under changing weather conditions.

Hardware Experiment and Comparison

Laboratory Setup and Design

A hardware laboratory test system of Fig. 8 is built for further investigation of the conventional and proposed MPPT algorithms. Figure 13 shows the testing system with the following setups. (1) An Agilent E4360A solar simulator is used to represent an actual PV array (KT, 2015). The solar simulator can generate real output voltage and current relation that is equivalent to a practical PV panel or array. By using the solar simulator, it is possible to repeat the same solar irradiation condition to test and compare different MPPT algorithms through a hardware experiment that is otherwise impossible. Another advantage is that the maximum output power of the simulated PV array can be calculated based on the experiment settings so that one can determine whether a MPPT algorithm is effective in a hardware experiment. Due to these reasons, solar simulators have been widely used by many researchers around the world for evaluation of a PV control system (Brito *et al*., 2011). (2) The dc/dc converter is built by using a LabVolt MOSFET power converter. (3) The capacitor connected to the output terminal of the simulator is formed by several LabVolt capacitors in parallel. (4) A smoothing inductor is employed for the dc/dc converter. (5) The solar simulator is controlled by a dSPACE digital control system (dSPACE, 2014). The control system collects output voltage and current signals of the solar simulator and sends a control signal to the converter based on control demands generated by different MPPT algorithms. Although the dSPACE system is not a digital device used for practical applications, it is a digital control system based on modern DSP chips (Rubaai *et al*., 2007). Using the dSPACE system, a MPPT digital controller can be quickly built and tested before converting it to a practical digital control device.

Experiment Analysis and Comparison

The rated values of the hardware experiment system (Fig. 13), including the power converter and the PV simulator, are different from those used in the computational experiment (Fig. 8). In general, the rating of the hardware experiment system is lower than the rating of a practical PV array. Therefore, parameters of the MPPT controllers must be returned. To ensure that the controllers work properly, the retuned MPPT algorithms for both the conventional and proposed techniques are evaluated in simulation first before the hardware experiment, where the simulation time step for the controllers is the same as the sampling time used in the dSPACE digital control system. Another big challenge, that is different from the simulation, is that noises are more significant than expected. One strategy to reduce the noises is to increase the strength of the measured signals.

Because of the noises, it is very hard to tune the MPPT parameters for IC and SF algorithms, especially for the SF algorithm. This is due to the fact that a noise can result in a high notch in the calculated power during the next sampling time, causing a large variation in power derivative and thus affecting the stability of the SF algorithm. However, for the proposed H-PI algorithm, a stable MPPT algorithm is much easier to obtain. The test sequence is scheduled as the following with $t = 0$ s as the starting point for data recording. Around $t = 20$ s, there is an increase of the solar irradiation. A small increase of the solar irradiation appears near $t = 40$ s. Close to $t = 60$ s, there is a large decrease of the irradiation. At about $t = 80$ s, the sequence repeats itself. The PV simulator voltage and current are not only collected by the dSPACE system but also monitored by oscilloscopes and/or meters. Figure 14 shows the captured maximum power by all the three algorithms. Again, the proposed H-PI approach has the best performance because for the proposed H-PI approach, the power derivative is smoothly processed before it is applied to the PI controller. In addition, the PI controller can response much faster than an open-loop scheme.

DOI: 10.3844/ajeassp.2016.755.769

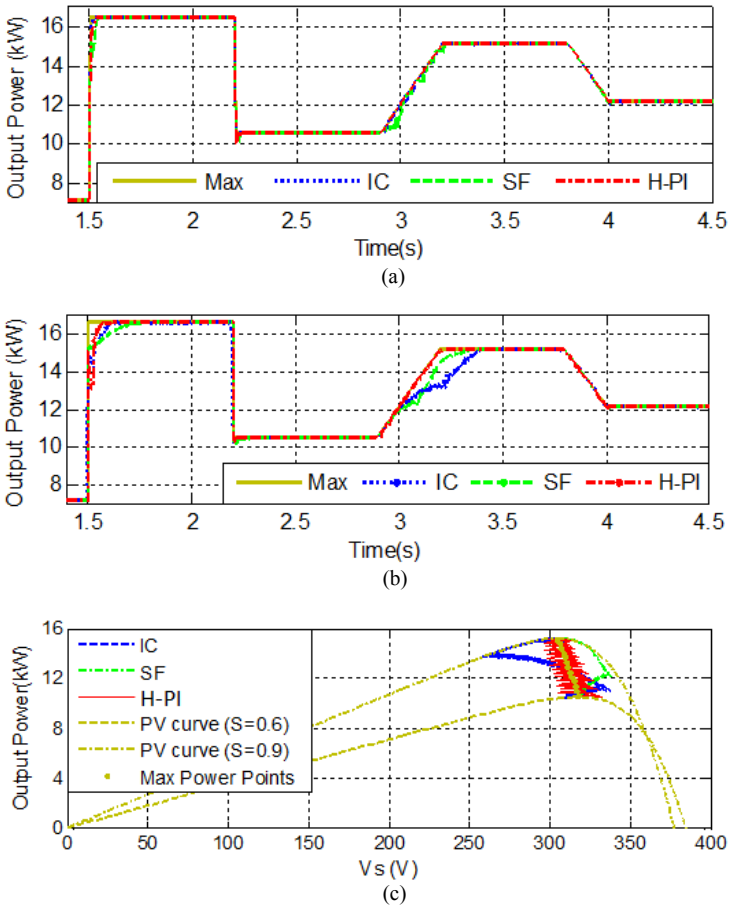

Fig. 11. MPPT comparison with different sampling rates (a) 1 ms per sample (b) 10 ms per sample (c) Power Vs. voltage locus at the increasing slope change (10 ms)

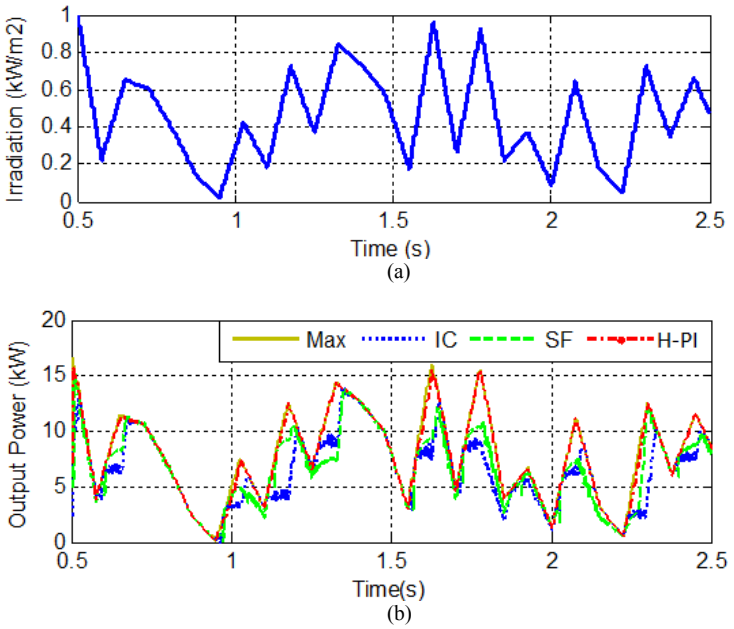

Fig. 12. MPPT comparison under variable solar irradiance conditions (a) Variable solar irradiance levels (b) PV array maximum and captured powers

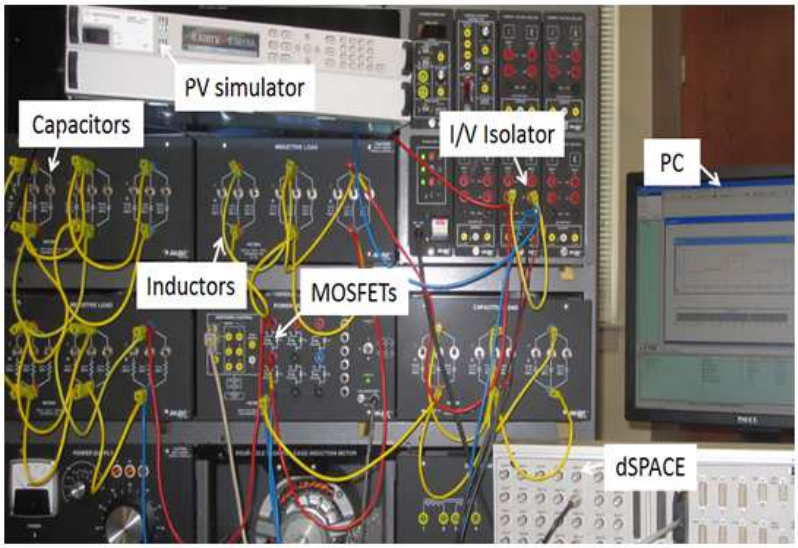

Fig. 13. Hardware experiment setup for evaluation of MPPT algorithms

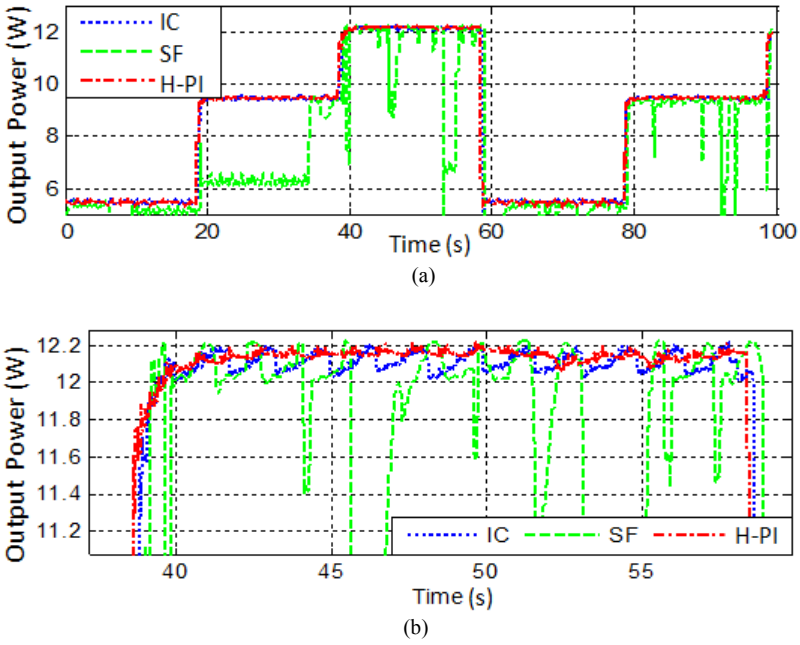

Fig. 14. Hardware experiment of captured maximum power using conventional and proposed MPPT algorithms (a) Captured output power in a long time range (b) A zoom-in of the captured output power

Conclusion

This paper proposes a fast and robust MPPT technique and compares it with typical conventional MPPT techniques used in solar PV industry. Among the three most popular conventional MPPT methods (IC, fixed step P&O and adaptive P&O), the IC and fixed step P&O methods have continuous oscillation even when the solar irradiation level is constant in the power converter switching environment; the adaptive P&O technique has small oscillation if the solar irradiation level is stable. For the proposed MPPT approach, it has the least oscillation and the highest stability.

The sampling rate influences the selection of the perturbation rate. This result indicates that proper selection of the sampling rate and perturbation step is important. If the sampling rate is too slow, a stable and reliable MPPT would be hard to achieve. Again, the

proposed method is more stable and reliable under different sampling rate conditions.

Under the variable irradiation levels, the proposed H-PI approach has better performance than conventional methods, indicating that the derivative of PV array terminal power Vs. voltage is valuable in capturing and tracking maximum power of a PV array under variable weather conditions. The comparison between the traditional and proposed adaptive methods shows that the hyperbolic processing of the derivation is important for high performance of a solar PV system.

In the hardware experiment, the unexpected noises would drastically influence the power increment or power derivative calculation in the next perturbation step. Because of the noises, it is very hard to tune the MPPT parameters for IC and SF algorithms, especially for the SF algorithm. However, for the proposed H-PI approach, the power derivative is smoothly processed before it is applied to the PI controller; in addition, the PI controller can response much faster than an open-loop scheme. The comparison demonstrates that the proposed H-PI approach is much easier to tune and has the best performance.

Funding Information

The authors have no support or funding to report.

Author's Contributions

Huiying Zheng: Made considerable contributions to acquisition of data and Analysis and interpretation of data. Contributed in drafting the article. Give final approval of the version to be submitted and any revised version.

Shuhui Li: Made considerable contributions to conception and design. Contributed in reviewing the article critically for significant intellectual content. Give final approval of the version to be submitted and any revised version.

Ethics

This article is original and contains unpublished material. The corresponding author confirms that all of the other authors have read and approved the manuscript and no ethical issues involved.

References

Abdelsalam, A. and A. Massoud, 2011. High-performance adaptive perturb and observe MPPT technique for photovoltaic-based microgrids. IEEE Trans. Power. Electron., 26: 1010-1021. DOI: 10.1109/TPEL.2011.2106221

Al-Amoudi, A. and L. Zhang, 1998. Optimal control of a grid-connected PV system for maximum power point tracking and unity power factor. 7th International Conference on Power Electronics and Variable Speed Drives, Sept. 21-23, IEEE Xplore Press, London, pp: 80-85. DOI: 10.1049/cp:19980504

ATSRD, 2011. Air temperature and solar radiation data.

Bao, K., S. Li and H. Zheng, 2012. Battery charge and discharge control for energy management in EV and utility integration. Proceedings of IEEE Power and Energy Society General Meeting, Jul. 22-26, IEEE Xplore Press, San Diego, CA., pp: 1-8. DOI: 10.1109/PESGM.2012.6344719

Brito, M.A.G., G.J. Luigi, L.P. Sampaio, A.M. Guilherme and C.A. Canesin, 2011. Evaluation of the main MPPT techniques for photovoltaic applications. IEEE Trans. Indust. Electron., 60: 1156-1167. DOI: 10.1109/TIE.2012.2198036

Carrasco, J.M., L.G. Franquelo, J.T. Bialasiewicz, E. Galván and R.C.P. Guisado *et al*., 2006. Power-electronic systems for the grid integration of renewable energy sources: A survey. IEEE Trans. Ind. Electron., 53: 1002-1016. DOI: 10.1109/TIE.2006.878356

Chedid, R., H. Akiki and S. Rahman, 1998. A decision support technique for the design of hybrid solar-wind power systems. IEEE Trans. Energy Convers., 13: 76-83. DOI: 10.1109/60.658207

dSPACE, 2014. DS1103 PPC controller board-powerful controller board for rapid control prototyping. dSPACE.

Esram, T. and P.L. Chapman, 1995. Comparison of photovoltaic array maximum power point tracking techniques. IEEE Trans. Energy Convers., 22: 439-449. DOI: 10.1109/TEC.2006.874230

Faranda, R. and S. Leva, 2008. Energy comparison of MPPT techniques for PV Systems. WSEAS Trans. Power Syst., 3: 446-455.

Faranda, R., S. Leva and V. Maugeri, 2008. MPPT techniques for PV systems: Energetic and cost comparison. Proceedings of the IEEE Power and Energy Society General Meeting-Conversion and Delivery of Electrical Energy in the 21st Century, Jul. 20-24, IEEE Xplore Press, Pittsburgh, PA., pp: 1-6. DOI: 10.1109/PES.2008.4596156

Faranda, R., S. Leva and V. Maugeri, 2008. MPPT techniques for PV systems: Energetic and cost comparison. Proceedings of the IEEE Power and Energy Society General Meeting-Conversion and Delivery of Electrical Energy in the 21st Century, IEEE Xplore Press, pp: 1-6. DOI: 10.1109/PES.2008.4596156

Femia, N., D. Granozio, G. Petrone, G. Spaguuolo and M. Vitelli, 2006. Optimized one-cycle control in photovoltaic grid connected applications. IEEE Trans. Aerosp. Electron. Syst., 2: 954-972. DOI: 10.1109/TAES.2006.248205

Femia, N., G. Petrone, G. Spagnuolo and M. Vitelli, 2005. Optimization of perturb and observe maximum power point tracking method. IEEE Trans. Power Electron., 20: 963-973. DOI: 10.1109/TPEL.2005.850975

Femia, N., G. Petrone, G. Spagnuolo and M. Vitelli, 2009. A technique for improving P&O MPPT performances of double-stage grid-connected photovoltaic systems. IEEE Trans. Ind. Electron., 56: 4473-4482. DOI: 10.1109/TIE.2009.2029589

Hussein, A., K. Hirasawa, J. Hu and J. Murata, 2002. The dynamic performance of photovoltaic supplied dc motor fed from DC-DC converter and controlled by neural networks. Proceedings of the International Joint Conference on Neural Networks, IEEE Xplore Press, May 12-17, Honolulu, HI., pp: 607-612. DOI: 10.1109/IJCNN.2002.1005541

Joerissen, L., J. Garche and C. Fabjan, 2004. Possible use of vanadium redox-flow batteries for energy storage in small grids and stand-alone photovoltaic systems. J. Power Sources, 127: 98-104. DOI: 10.1016/j.jpowsour.2003.09.066

KT, 2015. Keysight E4360: Modular solar array simulators. Keysight Technologies.

Khaehintung, N., K. Pramotung, B. Tuvirat and P. Sirisuk, 2004. RISC-microcontroller built-in fuzzy logic controller of maximum power point tracking for solar-powered light-flasher applications. Proceedings of the 30th Annual Conference of IEEE Industrial Electronics Society, Nov. 2-6, IEEE Xplore Press, pp: 2673-2678. DOI: 10.1109/IECON.2004.1432228

Kobayashi, K., H. Matsuo and Y. Sekine, 2004. A novel optimum operating point tracker of the solar cell power supply system. Proceedings of the IEEE 35th Annual Power Electronics Specialists Conference, Jun. 20-25, IEEE Xplore Press, pp: 2147-2151. DOI: 10.1109/PESC.2004.1355451

Li, S., T.A. Haskew, K.A. Williams and R.P. Swatloski, 2012. Control of DFIG wind turbine with direct-current vector control configuration. IEEE Trans. Sustain. Energy, 3: 1-11. DOI: 10.1109/TSTE.2011.2167001

Li, S., T.A. Haskew, Y. Hong and L. Xu, 2011. Direct-current vector control of three-phase grid-connected rectifier-inverter. Electric Power Sys. Res., 81: 357-366. DOI: 10.1016/j.epsr.2010.09.011

Lorenzo, E., G. Araujo, A. Cuevas, M. Egido and J. Miñano *et al*., 1994. Solar Electricity: Engineering of Photovoltaic Systems. 1st Edn., PROGENSA, Sevilla, ISBN-10: 8486505550, pp: 316.

Masters, G.M., 2004. Renewable and Efficient Electric Power Systems. 1st Edn., John Wiley and Sons, Hoboken, ISBN-10: 0471280607, pp: 654.

Mastromauro, R.A., M. Liserre and A.D. Aquila, 2012. Control issues in single-stage photovoltaic systems: MPPT, current and voltage control. IEEE Trans. Indust. Informat., 8: 241-254. DOI: 10.1109/TII.2012.2186973

Midya, P., P.T. Krein, R.J. Turnbull, R. Reppa and J. Kimball, 1996. Dynamic maximum power point tracker for photovoltaic applications. Proceedings of the 27th Annual IEEE Power Electronics Specialists Conference, Jun. 23-27, IEEE Xplore Press, Baveno, pp: 1710-1716. DOI: 10.1109/PESC.1996.548811

Mills, A., M. Ahlstrom, M. Brower, A. Ellis and R. George *et al*., 2011. Dark shadows. IEEE Power Energy Magaz., 9: 33-41. DOI: 10.1109/MPE.2011.940575

Nelson, J., 2003. The Physics of Solar Cells. 1st Edn., Imperial College Press, London, ISBN-10: 1860943497, pp: 363.

Noguchi, T., S. Togashi and R. Nakamoto, 2002. Short-current pulse-based maximum-power-point tracking method for multiple photovoltaic-and-converter module system. IEEE Trans. Ind. Electron., 49: 217-223. DOI: 10.1109/41.982265

ORTT, 2003. Real-time modeling tools: RT-Events^{TM}. Opal-RT Technologies.

Otieno, C., G. Nyakoe and C. Wekesa, 2009. A neural fuzzy based maximum power point tracker for a photovoltaic system. Proceedings of the IEEE AFRICON, Sept. 23-25, IEEE Xplore Press, Nairobi, pp: 1-6. DOI: 10.1109/AFRCON.2009.5308552

Rubaai, A., A.R. Ofoli and D. Cobbinah, 2007. DSP-based real-time implementation of a Hybrid H ∞ adaptive fuzzy tracking controller for servo-motor drives. IEEE Trans. Indust. Applic., 43: 476-484. DOI: 10.1109/TIA.2006.889904

Sun, X., W. Wu, X. Li and Q. Zhao, 2002. A research on photovoltaic energy controlling system with maximum power point tracking. Proceedings of the Power Conversion Conference, Apr. 2-5, IEEE Xplore Press, Osaka, pp: 822-826. DOI: 10.1109/PCC.2002.997626

Szabados, B. and F. Wu, 2008. A maximum power point tracker control of a photovoltaic system. Proceedings of the IEEE Instrumentation and Measurement Technology Conference Proceeding, May 12-15, IEEE Press, Vancouver BC., pp: 1074-1079. DOI: 10.1109/IMTC.2008.4547198

Veerachary, M., T. Senjyu and K. Uezato, 2003. Neural-network-based maximum-power-point tracking of coupled-inductor interleaved-boost-converter-supplied PV system using fuzzy controller. IEEE Trans. Indust. Electron., 50: 749-758. DOI: 10.1109/TIE.2003.814762

Wu, W., N. Pongratananukul, W. Qiu, K. Rustom and T. Kasparis *et al*., 2003. DSP-based multiple peak power tracking for expandable power system. Proceedings of the 18th Annual IEEE Applied Power Electronics Conference and Exposition, Feb. 9-13, IEEE Xplore Press, Miami Beach, FL, USA., pp: 525-530. DOI: 10.1109/APEC.2003.1179263

Yu, Z., 2007. Study of MPPT technique based on fuzzy logic control in PV system. Huazhong University of Science and Technology, Wuhan.